

## Effects of Photon-Momentum and Magnetic-Field Reversal on the Far-Infrared Electric-Dipole Spin Resonance in InSb

M. Dobrowolska,<sup>(a)</sup> Y. Chen, J. K. Furdyna, and S. Rodriguez

*Department of Physics, Purdue University, West Lafayette, Indiana 47907*

(Received 5 May 1983)

Far-infrared magnetotransmission experiments on *n*-type InSb in the parallel Voigt geometry ( $\vec{E} \parallel \vec{B} \perp \vec{k}$ ) conclusively demonstrate that the electric-dipole-excited spin resonance (EDSR) of conduction and donor-bound electrons in this material is allowed through lack of inversion symmetry. Quite unexpectedly for this geometry, the EDSR spectra also reveal an anomalous dependence on the *sign* of either  $\vec{B}$  or  $\vec{k}$ . It is shown, through time-reversal-symmetry arguments, that the above behavior represents an explicit contribution of the photon momentum to the dielectric response function.

PACS numbers: 78.20.Ls, 61.50.Em, 71.70.-d, 76.40.+b

In our far-infrared measurements of the electric-dipole spin resonance (EDSR) in *n*-type InSb, carried out in the parallel Voigt geometry ( $\vec{E} \parallel \vec{B}$ ), we have observed striking changes in the EDSR intensity produced by reversing the magnetic field direction. We found this result extremely surprising, because in the above geometry the response of the medium is described by a *diagonal* element of the dielectric tensor, which by simple symmetry arguments must remain invariant under magnetic-field reversal *unless* the effect of the wave vector of the propagating light is included.<sup>1</sup> The observed behavior must therefore represent a manifestation of time-reversal-symmetry effects associated with the small but finite contributions of the photon momentum to the response function of the medium. Qualitatively similar effects due to the finite photon momentum were observed in magneto-optical studies of exciton spectra in CdS<sup>2</sup> and CuBr.<sup>3</sup>

EDSR measurements were performed by far-infrared (FIR) transmission at a series of fixed wavelengths ( $\lambda = 96.5, 118.8, 163,$  and  $251.1 \mu\text{m}$ ) and as a function of magnetic field. The FIR radiation was generated by an optically pumped FIR laser (Apollo model 118). We used oriented crystals of *n*-type InSb with electron concentration ranging from  $1.6 \times 10^{14}$  to  $4.7 \times 10^{15} \text{ cm}^{-3}$ . The samples were cut in the form of plane-parallel disks (7 mm diam, 2 to 4.5 mm thick), the sample faces being either (100), (110), (111), or (112) planes. The samples were mounted in a Janis "supervaritemp" optical Dewar at the center of a split-coil 6-T superconducting solenoid, which permitted experiments in both the Faraday and the Voigt geometries. We shall focus here on the longitudinal Voigt geometry ( $\vec{E} \parallel \vec{B} \perp \vec{k}$ , where  $\vec{E}$  and  $\vec{k}$  are the polarization and the wave vector of propagating light, respectively, and  $\vec{B}$

is the dc magnetic field), which provides the strongest EDSR signal as well as the clearest and most direct arguments for the observed time-reversal effects. The intensity of the parallel Voigt EDSR was measured as a function of the angle between  $\vec{B}$  and the crystal axes. In order to rotate the sample, the constraints of our system required us to remove it from the Dewar, each new orientation being checked under a microscope. This procedure was quite tedious but very reliable and reproducible to  $\pm 2^\circ$ .

The electric-dipole-forbidden spin-resonance transition is allowed in the presence of spin-orbit coupling, when the selection rules which normally forbid these transitions are relaxed as a result of wave function mixing through either  $\vec{k} \cdot \vec{p}$  interaction (sometimes referred to simply as "nonparabolicity"),<sup>4</sup> inversion asymmetry,<sup>5,6</sup> or warping.<sup>6</sup> Of these, only inversion asymmetry allows the EDSR transition in the parallel Voigt geometry. Our experimental results clearly show that EDSR is actually strongest in this geometry and that it displays the anisotropy characteristic to inversion asymmetry.<sup>5</sup> While earlier investigations, carried out in other geometries, have ascribed the occurrence of EDSR in InSb to nonparabolicity,<sup>7</sup> we conclude that the dominant mechanism allowing this transition in InSb is inversion asymmetry.

Figure 1 presents the dependence of the EDSR absorption coefficient  $\alpha$  on the angle between the direction of  $\vec{B}$  and the crystallographic axes, obtained at  $118.8 \mu\text{m}$  in the Voigt  $\vec{E} \parallel \vec{B}$  geometry for a sample with faces in the (110) plane. Note the strong angular dependence of the data, and the systematic difference of the absorption coefficient corresponding to opposite field directions, indicated by black and white circles, respectively. The dashed curves are guides for the eye

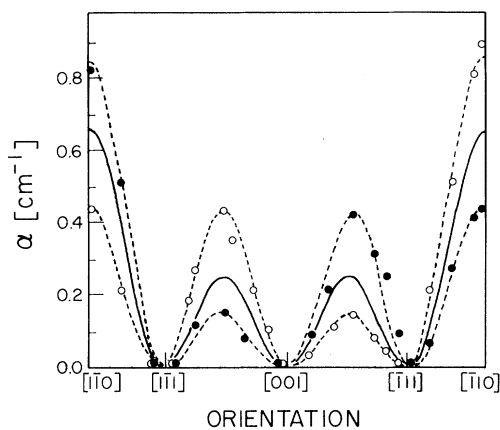


FIG. 1. Intensity of EDSR as a function of orientation of  $\vec{B}$  in the (110) plane, for  $\vec{k} \parallel [110]$ . Black and white circles correspond to opposite signs of  $\vec{B}$ , respectively. The solid line is the theoretical angular dependence of EDSR (from Ref. 5) normalized to the average of  $\alpha$  for  $+B$  and  $-B$  for  $\vec{B} \parallel [1\bar{1}0]$ . The data were observed at 4.5 K at  $118.8 \mu\text{m}$  on  $n$ -type InSb ( $n = 2.3 \times 10^{14} \text{ cm}^{-3}$ ), 4.5 mm thick.

connecting experimental points. The solid curve shows the angular dependence of the resonance intensity predicted for the inversion-asymmetry mechanism for this configuration.<sup>5</sup> This curve is normalized to the average experimental value for  $+B$  and  $-B$  for the  $[1\bar{1}0]$  direction. The agreement between experimental and theoretical angular dependence of the nodes and maxima of the EDSR indicates that the dominant mechanism allowing this transition is inversion asymmetry. Being aware of the fact that strain can enhance EDSR in InSb,<sup>8</sup> we have taken great care to mount samples in a strain-free manner, and have examined the anisotropy over  $360^\circ$  to ascertain that there exist no preferred directions other than those associated with the cubic symmetry.

A detailed analysis of the angular dependence of EDSR in InSb for this and other configurations will be published at a later date. Here we wish to focus on the behavior of EDSR observed on reversing the magnetic field, which we ascribe to the effect of photon momentum. To illustrate the symmetry properties of this effect, consider data obtained on a sample with (110) faces, in a sequence of configurations shown in Fig. 2. Figure 2(a) shows the EDSR signal for  $\vec{B} \parallel [1\bar{1}0]$  (in the face of the sample), with  $\vec{k} \parallel [110]$  (normal to the sample). Figure 2(b) represents EDSR when the sample is rotated  $180^\circ$  about  $\vec{k}$ ; Fig. 2(c) is for the sample rotated  $180^\circ$  about  $\vec{B}$  (flipped front to back), without changing the direction of  $\vec{k}$ ; Fig. 2(d) is observed for the sample rotated

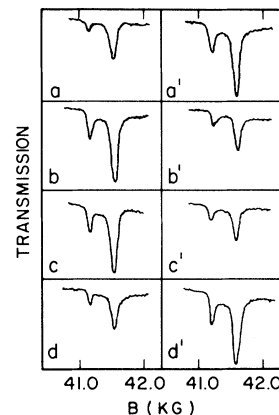


FIG. 2. Symmetry characteristics of EDSR in  $n$ -InSb, observed in the parallel Voigt geometry at  $118.8 \mu\text{m}$  and 4.5 K. The sample faces are in the (110) plane, sample thickness is 4.5 mm, and electron concentration  $n = 2.3 \times 10^{14} \text{ cm}^{-3}$ . (a) EDSR for  $\vec{B} \parallel [1\bar{1}0]$ ,  $\vec{k} \parallel [110]$ ; (b) the sample has been rotated by  $180^\circ$  about  $\vec{k}$  relative to (a); (c) the sample was rotated by  $180^\circ$  about  $\vec{B}$  relative to (a); (d) it was rotated by  $180^\circ$  about  $\vec{k} \times \vec{B}$  relative to (a). The sequence (a')-(d') corresponds to configurations (a)-(d), respectively, but with the magnetic field reversed. In each resonance doublet the higher-field, stronger line is the free-electron EDSR, and the weaker line is EDSR of donor-bound electrons.

$180^\circ$  about  $\vec{k} \times \vec{B}$  (in this case flipped front to back about the  $[001]$  cubic axis). Figures 2(a')-2(d') represent EDSR obtained with field reversed relative to 2(a)-2(d), respectively. The scale is identical for all data in Fig. 2. The following features emerge from the figure:

(1) The intensity of EDSR changes quite strongly (by a factor about 2) when the direction of the magnetic field is reversed relative to the crystal axes. This is observed by reversing the field itself [compare, e.g., Figs. 2(a) and 2(a')] or by rotating the sample by  $180^\circ$  about  $\vec{k}$  while keeping  $\vec{B}$  fixed in the laboratory frame [compare Figs. 2(a) and 2(b)].

(2) It is easily shown that rotating the sample by  $180^\circ$  about  $\vec{B}$  is equivalent to reversing the direction of  $\vec{k}$  while keeping  $\vec{B}$  fixed relative to the crystal directions. A change in EDSR intensity similar to that which takes place on reversing  $\vec{B}$  is observed when  $\vec{k}$  is reversed in this manner [compare Figs. 2(a) and 2(c)].

(3) Rotating the sample about  $\vec{k} \times \vec{B}$  is equivalent to reversing the direction of *both*  $\vec{k}$  and  $\vec{B}$  with respect to the sample. This operation leaves the EDSR intensity invariant [compare Fig. 2(a) with Fig. 2(d); Fig. 2(a') with Fig. 2(d')].

The dielectric response tensor  $\vec{\epsilon}$  which describes the above results must ultimately comply with the Onsager relations. In the local limit (i.e., when  $\vec{\epsilon}$  is independent of the wave vector  $\vec{k}$ ), Onsager's relations require that

$$\epsilon_{ij}(\omega, \vec{B}) = \epsilon_{ji}(\omega, -\vec{B}). \quad (1)$$

Since the dielectric response in the parallel Voigt geometry (for  $\vec{B} \parallel \hat{z}$ ) is described by  $\epsilon_{zz}$ , Eq. (1) immediately implies that in this geometry EDSR cannot depend on the *sign* of  $B$ . Thus, in order to understand the behavior illustrated in Fig. 2, we must introduce the nonlocal dielectric tensor  $\vec{\epsilon}(\omega, \vec{k}, \vec{B})$ . In this case the Onsager relations require that

$$\epsilon_{ij}(\omega, \vec{k}, \vec{B}) = \epsilon_{ji}(\omega, -\vec{k}, -\vec{B}). \quad (2)$$

Writing  $\epsilon_{ij}(\omega, \vec{k}, \vec{B})$  in a power series,<sup>1</sup>

$$\epsilon_{ij}(\omega, \vec{k}, \vec{B}) = \epsilon_{ij}(\omega) + i\gamma_{ijl}k_l + \alpha_{ijl}B_l + \beta_{ijlm}B_lk_m + \delta_{ijlm}B_lB_m + \dots, \quad (3)$$

we can see immediately that now

$$\begin{aligned} \epsilon_{zz}(\omega, \vec{k}, \vec{B}) &= \epsilon_{zz}(\omega, -\vec{k}, -\vec{B}) \\ &\neq \epsilon_{zz}(\omega, \vec{k}, -\vec{B}) = \epsilon_{zz}(\omega, -\vec{k}, \vec{B}), \end{aligned} \quad (4)$$

as a result of the term  $\beta_{ijlm}B_lk_m$ . It can be shown that such a term will exist only when the crystal lacks a center of inversion.<sup>1</sup>

The general properties of  $\beta_{ijlm}$  have been described in Ref. 1. We have examined this contribution for crystals with  $T_d$  symmetry (such as InSb). For example, for  $\vec{B}$  in the (110) plane,  $\vec{k} \parallel [110]$  direction, the term  $\beta_{ijlm}B_lk_m$  leads to a contribution to  $\epsilon_{zz}$  of

$$\Delta\epsilon_{zz} = \frac{1}{2}\beta_{44}'kB \sin\theta(3\cos^2\theta - 1), \quad (5)$$

where  $\beta_{44}'$  is a parameter describing the antisymmetric part of  $\beta_{ijlm}$  with respect to  $l$  and  $m$ ,<sup>1</sup> and  $\theta$  is the angle between  $\vec{B}$  and  $[001]$ . This is in exact agreement with the asymmetry between the data for  $+B$  and  $-B$  displayed in Fig. 1.

We have also carried out EDSR measurements on samples with (100), (111), and (112) faces. All these samples contain at least one  $[1\bar{1}0]$  direction (or equivalent) in the sample plane, facilitating comparison. When  $\vec{B}$  was parallel to  $[1\bar{1}0]$  in the case of the (111) and (112) samples, a similar asymmetry was observed with respect to field reversal and/or sample rotation as that shown in Fig. 2. The results for the (100) sample were unique, however, in that for this case the dependence of EDSR on the wave vector vanished, as shown in Fig. 3. This is, again, completely con-

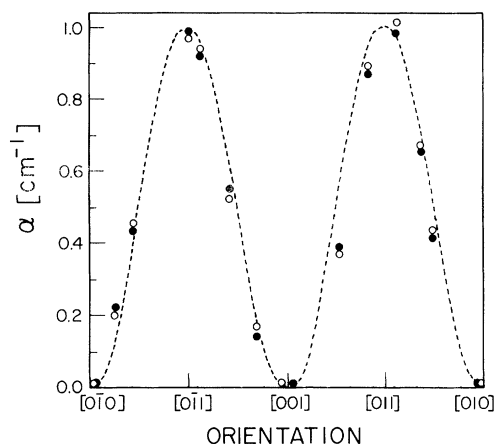


FIG. 3. Intensity of EDSR as a function of orientation of  $\vec{B}$  in the (100) plane. Black and white dots correspond to opposite field directions. The line shows the theoretical dependence for this plane (from Ref. 5), normalized to experimental data for  $\vec{B} \parallel [011]$ . The data were obtained at 4.5 K at  $118.8 \mu\text{m}$  on a sample with  $n = 3.6 \times 10^{14} \text{ cm}^{-3}$ , 4 mm thick.

sistent with the  $T_d$  symmetry, for which the contribution of  $\beta_{ijlm}B_lk_m$  can be shown to vanish identically when  $\vec{k}$  is along one of the cubic axes. This result can also be understood on intuitive grounds. In the case of a slab with (100) faces, a  $180^\circ$  rotation about  $\vec{k}$  (i.e., about the  $[100]$  direction) leaves the sample microscopically invariant. Since in the Voigt geometry such a rotation is equivalent to changing the sign of the magnetic field with respect to the sample, any effect related to reversing the magnetic field *in this plane* must vanish.

We found the time-reversal effects described above to be very reproducible in all the samples studied (a total of nine samples, with various electron concentrations, thicknesses, and orientations). The effects occurred as an inseparable part of the EDSR in the Voigt geometry at all temperatures ( $4.2 \text{ K} < T < 35 \text{ K}$ ) and FIR wavelengths ( $96.5 \mu\text{m} < \lambda < 251.1 \mu\text{m}$ ) where the experiments were performed. The time-reversal effects were present in EDSR of conduction electrons as well as donor-bound electrons, EDSR of the latter occurring in purer InSb as a result of freezeout (weaker line in Fig. 2). Since in InSb it is possible to distinguish physically between the  $[111]$  and  $[\bar{1}\bar{1}\bar{1}]$  directions by appropriate etching,<sup>9</sup> and thus to determine the direction of the magnetic field with respect to the zincblende lattice in absolute terms, we were able to ascertain that the time-reversal effects observed in *different* samples were consistent

among themselves. For example, EDSR was strong for  $\vec{E} \parallel [1\bar{1}0]$ ,  $\vec{k} \parallel [112]$  and weak for  $\vec{E} \parallel [1\bar{1}0]$ ,  $\vec{k} \parallel [\bar{1}\bar{1}2]$  in *all* (112) samples.

We have thus demonstrated, by time-reversal-symmetry arguments, that EDSR can serve as a vehicle for observing the small but finite photon momentum contributions to the macroscopic dielectric response function in acentric crystals.

It is likely that this effect arises from an interference between the matrix elements of the inversion asymmetry<sup>5</sup> and the Zeeman contributions to the Hamiltonian of the electron. We are presently investigating this microscopic mechanism.

The authors wish to thank A. K. Ramdas for illuminating discussions. The support of the National Science Foundation through Grant No. DMR79-23310 is gratefully acknowledged. We also thank the Purdue Central Laser Facility, supported by National Science Foundation-Materials Research Laboratory Grant No. DMR80-20249, where the FIR measurements were carried out.

<sup>(a)</sup>On leave from the Institute of Physics of the Polish

Academy of Sciences, 02-668 Warsaw, Poland.

<sup>1</sup>V. M. Agranovich and V. L. Ginzburg, *Spatial Dispersion in Crystal Optics and the Theory of Excitons*, Monograph No. 18 (Interscience, London, 1966), p. 11 ff and p. 176 ff.

<sup>2</sup>J. J. Hopfield and D. G. Thomas, *Phys. Rev. Lett.* **4**, 357 (1960).

<sup>3</sup>J. C. Merle, A. Bivas, C. Wecker, and B. Hönerlage, *Phys. Rev. B* **27**, 3709 (1983).

<sup>4</sup>Y. Yafet, in *Solid State Physics*, edited by F. Seitz and D. Turnbull (Academic, New York, 1963), Vol. 14, p. 1; V. I. Sheka, *Fiz. Tverd. Tela* **6**, 3099 (1964) [*Sov. Phys. Solid State* **6**, 2470 (1965)]. Note that the nonparabolicity-induced EDSR requires  $\vec{E} \perp \vec{B}$  and does not depend on the angle between  $\vec{B}$  and the crystal axes.

<sup>5</sup>E. I. Rashba and V. I. Sheka, *Fiz. Tverd. Tela* **3**, 1735, 1863 (1961) [*Sov. Phys. Solid State* **3**, 1257, 1357 (1961)].

<sup>6</sup>M. H. Weiler, *Solid State Commun.* **44**, 287 (1982); M. H. Weiler, R. L. Aggarwal, and B. Lax, *Phys. Rev. B* **17**, 3269 (1978).

<sup>7</sup>B. D. McCombe and R. J. Wagner, *Phys. Rev. B* **4**, 1285 (1971).

<sup>8</sup>F. Kuchar, R. Meisels, and M. Kriechbaum, in *Physics of Narrow Gap Semiconductors*, edited by E. Gornik *et al.*, Lecture Notes in Physics Vol. 152 (Springer-Verlag, Berlin, 1982), p. 197.

<sup>9</sup>H. C. Gatos and M. C. Lavine, *J. Phys. Chem. Solids* **14**, 169 (1960).